Friction and the Inverted Pendulum Stabilization Problem

Sue Ann Campbell

Department of Applied Mathematics,

University of Waterloo, Waterloo, ON N2L 3G1, Canada.

Stephanie Crawford and Kirsten Morris

Department of Applied Mathematics,

University of Waterloo, Waterloo, ON N2L 3G1, Canada.

Abstract

We consider an experimental system consisting of a pendulum, which is free to rotate 360 degrees, attached to a cart. The cart can move in one dimension. We study the effect of friction on the design and performance of a feedback controller, a linear quadratic regulator, that aim to stabilize the pendulum in the upright position. We show that a controller designed using a simple viscous friction model has poor performance - small amplitude oscillations occur when the controller is implemented. We consider various models for stick slip friction between the cart and the track and measure the friction parameters experimentally. We give strong evidence that stick slip friction is the source of the small amplitude oscillations. A controller designed using a stick slip friction model stabilizes the system, and the small amplitude oscillations are eliminated.

Keywords: inverted pendulum, friction, feedback control, stability analysis.

INTRODUCTION

Although friction, which dissipates energy in a system, would seem to be a stabilizing force, it has been shown [1] that underestimating the size of the friction coefficient may sometimes lead to instability in a feedback control system. For example, unmodelled friction effects were considered to be the cause of failure of a feedback controller to stabilize a three link inverted pendulum system [2]. Friction has also been associated with oscillatory behaviour. Friction generated limit cycles were shown in simulations of a simple cart system [3] and were observed experimentally in a balancing apparatus in [4]. Oscillatory behaviour was predicted theoretically in a balancing system with backlash [5]. Oscillatory behaviour about the equilibrium point has been attributed to unmodelled Coulomb friction in both single [6, 7] and double inverted pendulum [8] experimental systems.

Several approaches have been used to eliminate the problems due to unmodelled friction. Here we review the approaches that have been used in systems related to the physical problem we will study, the inverted pendulum. A more general review, including more complicated physical systems and other approaches for dealing with friction may be found in [9]. One approach is friction compensation: the addition of a feedback term $u = -F_{\text{fric}}$ where F_{fric} is an estimate of the neglected friction force. This approach has been shown to reduce the amplitude of the limit cycles associated with unmodelled friction in single [7] and double [8] inverted pendulum systems, however, it does not eliminate them entirely. Chang and Lee [10] use friction compensation and a disturbance observer to deal with unmodelled friction in their control of a bi-axial inverted pendulum. Although a very detailed friction model is used, a small amplitude limit cycle persists when the controller is applied to the experimental system. Eltohamy and Kuo [2] used cascaded controllers to overcome the failure of their linear quadratic regulator (LQR) controller, which was designed ignoring Coulomb friction, to stabilize a triple inverted pendulum. Their approach succeeded in maintaining the system in the upright position, but oscillations about the equilibrium point are present. Another approach is the use of robust control techniques. H_∞ control has been applied to both single [11] and double [12] inverted pendulum systems. These controllers were able to reduce the amplitude limit cycles associated with unmodelled friction, but do not eliminate them entirely.

Here we focus on a more direct approach, namely, using the best friction model available in

the design of the controller, rather than increasing the complexity of the controller in order to compensate for a design obtained using an inaccurate model. In fact, several of the studies above [2, 8] suggested that such an approach was needed to achieve better performance. We focus on a simple paradigm: the design of a controller to balance a pendulum in the inverted position. Generalizations to pendulum systems with more links and other more complicated control systems are readily apparent. Further, we focus on stabilizing the pendulum in the upright position. This is in contrast to the swing-up problem (e.g., [6, 13]), where one designs a controller to bring the pendulum close the upright pendulum and then employs a controller to stabilize it. Unmodelled friction effects seem to be more of a problem in the stabilization phase than in the swing-up phase [6, 14].

In particular, we will compare two models which combine the effect of viscous, sliding and static friction: the common static model with the Stribeck effect [9] and a dynamic model due to Canudas de Wit et al. [15]. We shall show both analytically and using numerical simulations that either model can account for the oscillations which occur when a controller designed using only viscous friction is applied to a system with all three components of friction. We shall then show, by numerical simulation and experiment, that incorporating the either of these friction model into the LQR design yields a controller with better performance. Finally we shall compare the robustness to delays of controllers designed with each of these friction models.

The plan of our article is as follows. The next section contains a description of our experimental setup and mathematical model including a review of the two friction models and a description of how we estimate the model parameters experimentally. In section 3 we present our results contrasting the situation when each friction model is used. and numerical simulations to study the stability of the up equilibrium point of the controlled system using the new friction models. In section 4 we design a new controller using the new friction models and show that it achieves better results. In section 5 we study the effect of time delay in the controller. Finally, in section 6 we summarize our work and draw some conclusions.

BACKGROUND

The experimental system we study is depicted schematically in Figure 1. In this system, a pendulum is attached to the side of a cart by means of a pivot which allows the pendulum

to swing in the xy-plane. A force $F(t)$ is applied to the cart in the x direction, with the purpose of keeping the pendulum balanced upright.

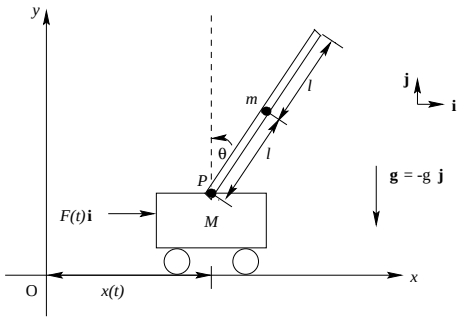

FIG. 1: Inverted Pendulum System

The equations of motion of the cart and pendulum from Figure 1 can be found using Hamilton's Principle. They are:

$$\begin{aligned} (M+m)\ddot{x}(t) - ml\sin\theta(t)\dot{\theta}(t)^2 + ml\cos\theta(t)\ddot{\theta}(t) &= F(t) + F_{\text{fric}}(t), \\ ml\cos\theta(t)\ddot{x}(t) - mgl\sin\theta(t) + \tfrac{4}{3}ml^2\ddot{\theta}(t) &= 0, \end{aligned} \tag{1}$$

where x is the position of the cart, θ is the pendulum angle, measured from the upright position, F is the force applied to the cart and F_{fric} is the force of friction between the cart and the track. The friction between the pendulum and the pivot is much smaller and thus we neglect it. The definitions of the parameters and their values are given in Table I.

TABLE I: Parameter Values for Experimental Setup

Parameter	Description	Value
M	mass of the cart	0.815 kg
m	mass of the pendulum	0.210 kg
l	distance from pivot to center of mass of the pendulum	0.305 m
g	gravitational constant	9.8 m/s^2
α	voltage to force conversion factor	1.719 N/volt
β	electrical resistance to force conversion factor	7.682 N-s/m

In our experimental system, supplied by Quanser Limited, the applied force is due to a motor in the cart and is given by

$$F(t) = \alpha V(t) - \beta\dot{x}(t), \tag{2}$$

where V is the voltage supplied to the motor, and the second term represents electrical resistance in the motor. The values of the constants α and β for the motor used in our experimental apparatus are given in Table I.

In [16], this system was studied assuming that the only kind of friction present was viscous friction, so that $F_{\text{fric}} = -\epsilon\dot{x}$. A more accurate model of the friction between the cart and the track should also include static and Coulomb (sliding) friction. By studying our experiment under the conditions of a voltage ramp, we determined that the transition from the cart being stationary to when it was moving was smoother than would be expected from a simple combination of static, Coulomb and viscous friction. This is known as the Stribeck effect [17]. We considered two models that incorporate this smoothing, described below. We will compare the effect of including each of these friction models in our model for the experimental system.

A common way to smooth the transition from stationary to moving is to add an exponential factor [9]. This leads to the first friction model that we use:

$$F_{\text{fric}} = \begin{cases} F_{\text{static}} & \text{if } \dot{x} = 0, \\ -(\mu_c + (\mu_s - \mu_c)e^{-(\frac{\dot{x}}{v_s})^\gamma})F_N \operatorname{sgn}(\dot{x}) - \epsilon\dot{x} & \text{if } \dot{x} \neq 0, \end{cases} \tag{3}$$

where $\mu_s,\ \mu_c, \epsilon$ are the coefficients of static, Coulomb and viscous friction, respectively, F_N is the magnitude of the normal force, v_s is called the Stribeck velocity and γ the form factor. Recall that static friction is given by

$$F_{\text{static}} = \begin{cases} -F_{\text{applied}} & \text{if } |F_{\text{applied}}| < \mu_s F_N \\ -\mu_s F_N \operatorname{sgn}(F_{\text{applied}}) & \text{if } |F_{\text{applied}}| \geq \mu_s F_N \end{cases}. \tag{4}$$

In our system the object is moving horizontally, so $F_N = (m + M)g$.

The values that we use for the various parameters in this model are given in Table II. To estimate μ_c and ϵ we applied a constant voltage to the cart and allowed it to reach a steady state (constant velocity). Given two values for the constant applied voltage, V, and corresponding constant final velocity, $\dot{x}$, one can use the steady state version of the equations of motion to solve for μ_c and ϵ. To estimate the value of the static friction coefficient μ_s, we followed the procedure of Armstrong-Hélouvry [18]. This consists of gradually increasing the voltage applied to the cart and measuring voltage (and hence force) necessary to make the cart start to move. The Stribeck parameters, ν_s and γ, were chosen by trial and error,

TABLE II: Parameters for Exponential Friction Model

Parameter	Description	Value
μ_s	coefficient of static friction	0.08610
μ_c	coefficient of Coulomb friction	0.04287
ϵ	coefficient of viscous friction	3 N-sec/m
v_s	Stribeck velocity	0.105 m/sec
γ	form factor	2

so that simulations of the model best matched experimental data. A force velocity plot for this friction model with the parameters we estimated may be found in [19, Figure 3].
In our analysis in the following sections, we will need the right hand side of our model to be differentiable so that we may linearize it about the origin. The term $\text{sgn}(\dot{x})$ in the above model is problematic as it is not continuous at 0. Instead of dropping this non-smooth term when linearizing as is commonly done, we will approximate it by a smooth function: $\tanh(\delta x)$ where δ is a large number. This has been proposed by other authors (e.g., [20]) to improve the efficiency of simulations of models with Coulomb friction. Whether such smooth approximations are a good representation of stick-slip friction is debatable [9]. Our goal is only to include some information about these important nonlinear terms in the controller design.

Dynamic Friction Model

The second model we use is due to Canudas de Wit et al. [15]. This model attempts to represent friction more physically by thinking of two surfaces making contact through elastic bristles. The main idea is that when a force is applied, the bristles will deflect like springs, which gives rise to the friction force. The friction force generated by the bristles is

$$F_{\text{fric}} = -(\sigma_1 + \epsilon)\dot{x} - \sigma_0 z \left(1 - \sigma_1 \frac{|\dot{x}|}{g(\dot{x})}\right), \tag{5}$$

where z is the average deflection of the bristles, and σ_0, σ_1 are the stiffness and damping coefficient and $g(\dot{x}) = (\mu_c + (\mu_s - \mu_c)e^{-(\frac{\dot{x}}{v_s})^\gamma})F_N$. The variation of z is modelled via:

$$\frac{dz}{dt} = \dot{x} - \sigma_0 \frac{|\dot{x}|}{g(\dot{x})} z. \tag{6}$$

Note that when $\dot{x}$ is constant, the bristle state z, and hence F_{fric}, approach constant values: $z = \frac{1}{\sigma_0} g(\dot{x}) \operatorname{sgn}(\dot{x})$ and $F_{\text{fric}} = -(\mu_c + (\mu_s - \mu_c)e^{-(\frac{\dot{x}}{v_s})^\gamma})F_N \operatorname{sgn}(\dot{x}) - \epsilon\dot{x}$. Thus, the steady state friction force is the same as that of the exponential friction model, Eqs. (3)–(4).

Since we have already determined the parameters for the exponential friction model (Table II), we only need to determine σ_0 and σ_1. To obtain these parameters, we started with values similar to those used in [15] and then adjusted them to fit the experimental data. The values we use are given in Table III. A force velocity plot for this friction model with

TABLE III: Parameters for Dynamic Friction Model

Parameter	Description	Value
σ_0	stiffness	121 N/m
σ_1	damping coefficient	70 N-sec/m

the parameters we estimated may be found in [19, Figure 5].

Note that this model also cannot be linearized about the origin due to the term involving $|\dot{x}|$. Thus we approximate $|\dot{x}|$ by a differentiable function. However, any such approximation will have derivative 0 when $\dot{x}$ is 0, so the terms involving $|\dot{x}|$ contribute nothing to the linearization.

LQR Controller Design

Regardless of the friction model chosen, if there is no applied force ($F(t) = 0$) system (1) will have two types of equilibrium points: one corresponding to the pendulum hanging straight down and one to the pendulum pointing straight upward. We will refer to these as the down and up equilibria, respectively. It is well known (see e.g. [16]) that when there is no applied force the down equilibrium point is stable and the up equilibrium point is unstable.

System (1) with applied force given by Eq. (2) and either friction model, can be written in first-order form, $\dot{\mathbf{x}} = \mathbf{f}(\mathbf{x})$, and linearized to obtain an equation of the form $\dot{\mathbf{x}} = A\mathbf{x} + BV(t)$,

where $V(t)$ is the applied voltage and $\mathbf{x}, A$ and B depend on the model used for friction in the physical system.

To determine how to choose $V(t)$ to stabilize the up equilibrium point, we solve a linear quadratic control problem as described in, for example, [21]. In particular, we use the linear quadratic cost functional

$$\inf_{V(t)\in L_2(0,\infty)} \int_0^\infty \left[\mathbf{x}(t)^T Q \mathbf{x}(t) + rV(t)^2\right] dt,$$

where the weights $Q \geq 0$ and $r > 0$ are chosen to reflect the relative importance of reducing the states $\mathbf{x}$ and the cost of the control V. The solution to this problem is the feedback law

$$V(t) = K \cdot \mathbf{x}(t), \tag{7}$$

where the gain K depends on the choice of the design parameters r, Q and (through A and B) on the choice of friction model. With this feedback law, the applied force in the system, Eq. (2), becomes

$$F(t) = \alpha K \cdot \mathbf{x}(t) - \beta \dot{x}(t) \tag{8}$$

Since our system is linear and single-input, the control weight r can be absorbed into the state weight Q and was set to 1. The state weight Q is chosen to penalize the positions heavily with small costs on the velocities. This choice of weights penalizes non-zero position so that the resulting controller will maintain the pendulum near the upright position. Reducing the velocities to zero is a secondary objective. This reasoning led to $Q = \text{diag}(5000, 3000, 20, 20)$ in [16]. We shall use this same Q throughout the paper.

FRICTION INDUCED LIMIT CYCLES

In [16] system (1) was considered with a simple viscous friction model $F_{fric} = \epsilon\dot{x}$ ($\epsilon = 2.1$). In this case, the state in the linearized model is $\mathbf{x} = (x, \theta, \dot{x}, \dot{\theta})$. An optimal linear quadratic design as described above leads to a feedback gain $K = [k_1, k_2, k_3, k_4] = [70.71, 142.5, 50.69, 26.98] = K_{\text{vis}}$. For system (1) with the viscous friction model and this control gain, the upright equilibrium point is asymptotically stable. However, when the controller was implemented in the experimental system, small oscillations resulted. In the following we will study system (1) with this controller, but with either the exponential

friction model or the dynamic friction model. We will show that the oscillations in the experiment can be reproduced in either model. This gives strong evidence that the oscillations are due to neglecting the stick slip friction when the controller was designed.

Consider our model (1) with the exponential friction model (3)–(4) with the applied force (8). This may be transformed to a first order equation $\dot{\mathbf{x}} = \mathbf{f}(\mathbf{x})$ with $\mathbf{x} = (x, \theta, \dot{x}, \dot{\theta})$. The linear (local) stability of the up equilibrium point is determined by the eigenvalues of the Jacobian of $\mathbf{f}$ evaluated at the equilibrium point, $\mathbf{x} = \mathbf{0}$.

For the parameter values of our experiment (Tables I and II) and the control gain $K = K_{\text{vis}}$, the Routh Hurwitz Criterion (e.g. [21]) shows that the Jacobian matrix has two eigenvalues with positive real parts if $\delta > 60.4$. Since we require that δ is large, this indicates that the up equilibrium is *unstable* for the system with the exponential friction model and the feedback control designed using the viscous friction model. This agrees with the fact that the experimental system did not settle into the equilibrium point. Further, for $60.4 < \delta \leq 241$, the eigenvalues with positive real parts occur in complex conjugates, which is consistent with the observation of oscillations in the physical system.

Numerical simulations of the full nonlinear system (1) with the exponential friction model (3)–(4), applied force (8) and the control gain $K = K_{\text{vis}}$, agree with the prediction of the linear analysis that the equilibrium point is unstable. Simulations which start close to the equilibrium point tend away from it and ultimately oscillate with constant amplitude. An example is shown in Figure 2, along with a typical experimental time trace. The simulation and the experiment exhibit oscillations with similar amplitude and frequency. (In Figure 2 and subsequent similar figures, the simulations have been shifted to overlap the experimental results, since the final position of the cart is arbitrary.)

Now consider our model (1) with the dynamic friction model (5)–(6), the applied force (8) and the control gain $K = K_{\text{vis}}$. This may be transformed to a first order equation $\dot{\mathbf{x}} = \mathbf{f}(\mathbf{x})$ with $\mathbf{x} = (x, \theta, \dot{x}, \dot{\theta}, z)$. We then calculate the Jacobian of $\mathbf{f}$ about the up equilibrium point, $\mathbf{x} = \mathbf{0}$.

Analysis of the corresponding characteristic equation, with the parameter values given in Tables I, II and III, shows that the eigenvalues are: 0, -118.42, -5.33, -0.14 ± 0.067. The zero eigenvalue is due to the state z which cannot be controlled by the control signal. The equilibrium points are not isolated, but come in lines, since the z coordinate can take any value. Since all the eigenvalues other than zero have negative real parts, the line of

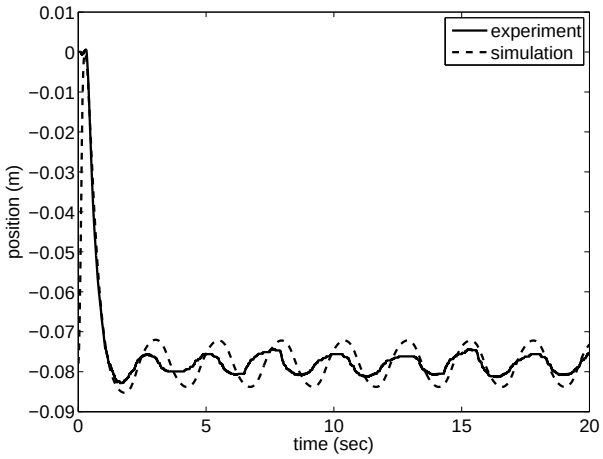

FIG. 2: Comparison of experiment with control gain $K = K_{\text{vis}}$ and simulation of pendulum cart system (1) with the same controller and the exponential friction model.

equilibrium points is *orbitally asymptotically stable*. This means that any initial condition close enough to the line will approach one of the points on the line [22, Theorem 4.3].
A numerical simulation of the full nonlinear system (1) with the dynamic friction model (5)–(6), the applied force (8) and the control gain $K = K_{\text{vis}}$ is shown in Figure 3(a) along with the results of a typical experiment using the same controller. The simulation agrees with the experiment in that they both show oscillations, however, the frequency and amplitude match is not as good as with the exponential friction model. This simulation result seems to differ from the analysis that the equilibrium point is orbitally asymptotically stable. However, this is clarified by the simulations shown in Figure 3(b). In this case, two initial conditions very close to zero are chosen and one can see that the smaller one goes asymptotically to the equilibrium point while the larger one goes the periodic solution. Thus it would appear that with the dynamic friction model the equilibrium point is orbitally asymptotically stable and coexists with a stable periodic orbit. Further, the basin of attraction of the equilibrium point is quite small, so most initial conditions lead to oscillations.

ELIMINATION OF LIMIT CYCLES BY NEW CONTROLLERS

In this section we will use the exponential and dynamic friction models to design new controllers that will stabilize the upright equilibrium point. The system (1) with applied force given by (2) and either of the friction models is written in first-order form and linearized

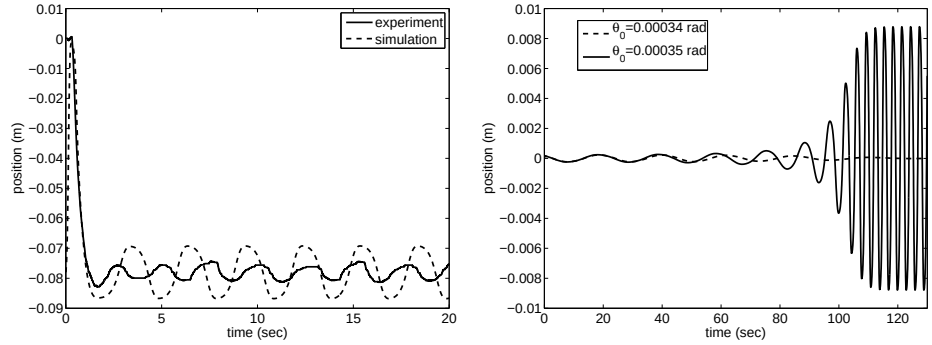

(a) (b)

FIG. 3: Simulations of pendulum cart system (1) with the dynamic friction model (5)–(6) and the control gain $K = K_{\text{vis}}$. (a) Initial angle is chosen for comparison with experiment. (b) Two initial angles very close to zero are chosen to illustrate the bistability between the equilibrium point and the periodic solution.

to obtain equations of the form

$$\dot{\mathbf{x}} = A\mathbf{x} + BV(t) \tag{9}$$

where $V(t)$ is the applied voltage and $\mathbf{x}$, A and B depend on the model (exponential or dynamic) used for friction. To determine how to choose $V(t)$ to stabilize the up equilibrium point, we solve a linear quadratic control problem as described in Section 2.

Controller for the Exponential Model

In this case, the state is $\mathbf{x} = (x, \theta, \dot{x}, \dot{\theta})$. Setting the slope parameter in the smooth approximation to the sgn function to be $\delta = 100$, we design the controller as discussed in section 2 and find the new feedback gain is $K = [70.71,\ 304.9,\ 143.3,\ 61.08] = K_{\text{exp}}$. Numerical simulations of the full nonlinear system (1) with the exponential friction model (3)–(4) confirm that the pendulum is stabilized in the inverted position by this controller. We implemented this controller in our experimental system and found that it did stabilize the system. An example experimental run and simulation are shown in Figure 4. The performance of the controlled system is considerably better than that obtained with the controller designed using the simple viscous friction model.

It is clear from the figure, however, that there remains some noise in the system. By running

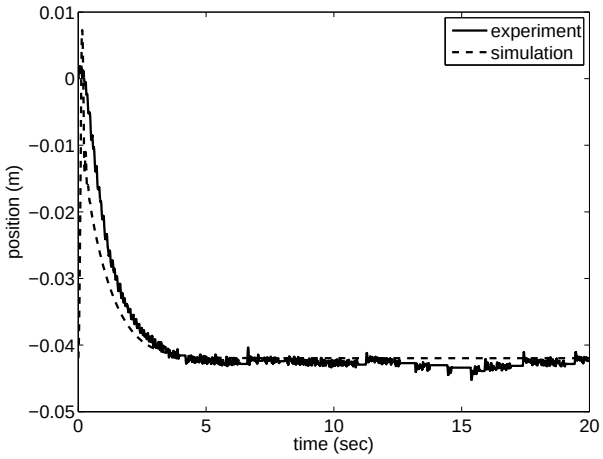

FIG. 4: Implementation of the controller based on the exponential friction model in the experiment (solid line) and in a numerical simulation of the system with initial condition $(x, \theta, \dot{x}, \dot{\theta}) = (0, 0.06 \text{ rad}, 0, 0)$ (dashed line).

a frequency analysis on the experiment and examining the experimental data at a finer scale, we determined that the most likely source of this noise was quantization error in the digital encoders used to measure the cart position and pendulum angle.

Controller for the Dynamic Model

Here $\mathbf{x} = (x, \theta, \dot{x}, \dot{\theta}, z)$. The matrices A, B are found by rewriting system (1), with $F(t) = 0$ and the friction model given by Eqs. (5)–(6), as a five dimensional first order system and then linearizing about the upright equilibrium.

Ideally, a control system should be *controllable*. For our system this means, roughly, that there exists a control signal $V(t)$ to control the system from any initial state to any final state. *Stabilizability* is a weaker property. System (9) is stabilizable if there exists some matrix K such that $A - BK$ has all eigenvalues with negative real parts. A stabilizable system can be controlled from any initial state to zero. The linear quadratic control problem can only be solved if the system is stabilizable (see, e.g., [21]). For system (9) to be stabilizable, the rank of $[(\lambda I - A) \;\; B]$ for any positive or zero eigenvalue λ of A must be 5 [21]. It is easily checked that this system is not stabilizable. This is due to the introduction of the additional "friction state" z. The model must undergo a transformation so that it becomes controllable

and stabilizable. Let $\mathbf{s} = U\mathbf{x}$ where U is the transformation matrix. Then the new model is given by:

$$\begin{aligned} \dot{\mathbf{s}} &= (UAU^{-1})\mathbf{s} + (UB)\mathbf{u} \\ &= \begin{bmatrix} A_c & A_{cu} \\ 0 & A_u \end{bmatrix} \begin{bmatrix} \mathbf{s}_c \\ \mathbf{s}_u \end{bmatrix} + \begin{bmatrix} B_c \\ 0 \end{bmatrix} V(t) \end{aligned} \tag{10}$$

The subsystem $\dot{\mathbf{s}}_c(t) = A_c\mathbf{s}_c(t) + B_cV(t)$ is controllable. We used the Matlab function `minreal`, to obtain a controllable subsystem of order 4 for our system. We then calculated the controller for the controllable subsystem, using the control weight $r = 1$ and the transformed state weight $Q' = \hat{U}^TQ\hat{U}$ where Q is as for the other models and $\hat{U}$ is 4×4 matrix formed by taking the first 4 rows and columns of U. We obtain $K' = [136.0, -124.0, -58.10, 288.9]$. This K' stabilizes the controllable subsystem. The feedback for the original system is $K = [K'\hat{U}, 0]$. Thus the new K is [85.08, 290.5, 136.0, 58.10, 0] = K_{dyn}. Linear analysis shows that with this controller the up equilibrium point is orbitally asymptotically stable.

Numerical simulations and experimental results, such as those shown in Figure 5, indicate that the controller stabilized the equilibrium point in nonlinear system. Again, the performance is considerably better than that of the controlled system obtained using the simple viscous friction model. As with the controller based on the exponential friction model, there remains some noise in the system. As discussed at the end of the previous subsection, this is likely due to the resolution of the sensors.

EFFECT OF TIME DELAY

As illustrated in the last section, the LQ controller designed with either friction model achieves stability of the upright equilibrium point. Another measure to compare them is their robustness with respect uncertainty. An important such uncertainty is time delay. The minimum time delay which causes the system to become unstable is directly related to the phase margin of the controlled system [21].

We assume that there is a time delay, $\tau > 0$, between when the variables used in the feedback law (7) are measured and when the voltage $V(t)$ is applied. Adding this delay to the model,

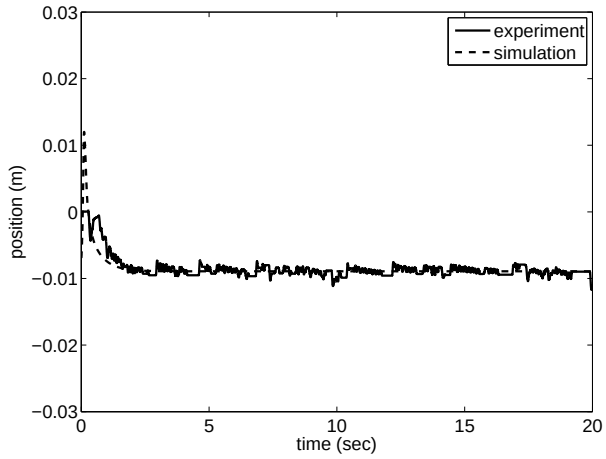

FIG. 5: Implementation of the controller based on the dynamic friction model in the experiment (solid line) and in a numerical simulation of the system with initial condition $(x, \theta, \dot{x}, \dot{\theta}) = (0, 0.02 \text{ rad}, 0, 0)$ (dashed line).

the applied force in (1) now becomes

$$F(t) = \alpha K \cdot \mathbf{x}(t - \tau) - \beta \dot{x}(t). \tag{11}$$

We wish to find the smallest time delay $\tau_c > 0$ that makes the upright equilibrium point of this system unstable. Rewriting the model as a first order system and linearizing about the upright equilibrium point yields the system $\dot{\mathbf{x}} = A\mathbf{x}(t) + E\mathbf{x}(t - \tau)$, where $\mathbf{x}$ and A and E depend on which friction model is used. The critical delay, τ_c, is the smallest delay such that the characteristic equation of the linearization has an eigenvalue with zero real part. More information on the theory of systems with time delay may be found in [23].

To study this experimentally, we implemented the feedback control based on one of the friction models, i.e., (11) with either $K = K_{\text{exp}}$ or $K = K_{\text{dyn}}$, in our experimental system.We then artificially increased the time delay using the computer system which implements the feedback control and observed how the behaviour of the system changed. Our initial conditions for the experiment are set manually, by holding the pendulum "close" to the upright position. They are given by

$$\mathbf{x}(t) = (0, \theta_0, 0, 0), \ -\tau \leq t \leq 0, \tag{12}$$

where $1 \leq \theta_0 \leq 5$ degrees.

Time Delay with the Exponential Friction Model

For the exponential model, $\mathbf{x} = [x, \theta, \dot{x}, \dot{\theta}]$, and A and E are easily calculated. See [19] for details. Using the parameters in Tables I and II and $\delta = 100$, we find that the critical time delay is $\tau_c \approx 0.1069$ seconds. Experimentally we observed that the upright equilibrium point was asymptotically stable until $\tau = 0.01$. For $0.01 < \tau < 0.025$ the experimental system exhibited oscillations about the upright equilibrium point, with amplitude that increased with τ. For $\tau \geq 0.025$, the pendulum fell down.

We performed numerical simulations of the nonlinear system (1) with the delayed force (11) and exponential friction model (3)–(4), using initial conditions (12) with $\theta_0 \leq 10$ deg. The numerical integration routine had difficulty dealing with initial conditions smaller than 0.06 degree due to the signum function. Thus we also performed simulations using the smooth approximation $\tanh(100\,\dot{x})$ for $\mathrm{sgn}(\dot{x})$ in Eq. (3). The results of the simulations are summarized in the top graph of Figure 6 with a zoom in shown in the bottom graph. Clearly, the simulation results match the experimental observations better than the theoretical prediction based on the linearization of the model with the smooth approximation to the signum function. For initial conditions with $\theta_0 > 0.1$ degree, the two sets of simulations give very similar results. For small enough initial conditions, the simulations with the smooth approximation show the delay where stability is lost matches the theoretical prediction from the linearization, as it should.

These results lead to two possible explanations for the discrepancy between the theoretical prediction and the experimental observations. The simplest is that while the smooth approximation is good enough to design a controller which stabilizes the system, it is not good enough for quantitative predictions of delay-induced instability. Alternatively, the simulations with the smooth approximation indicate that the discrepancy is because the equilibrium point is only locally asymptotically stable. We cannot verify this experimentally, since it is impossible to get the pendulum sufficiently close to the equilibrium point. However, we can conclude from both sets of simulations that the *effective* critical delay (i.e. the delay where stability will be lost with experimentally achievable initial conditions) is considerably less than that predicted by the linear stability analysis.

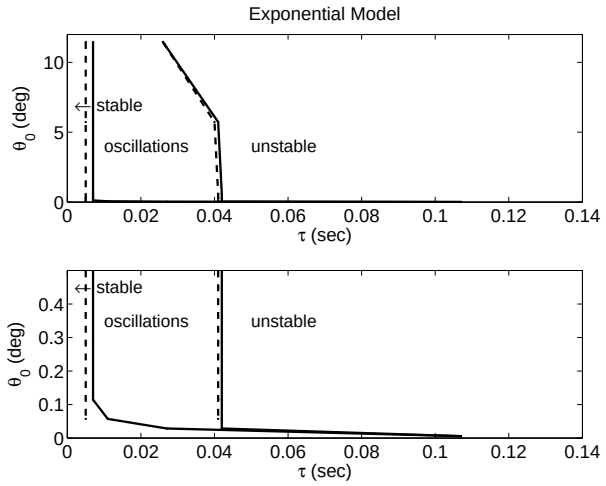

FIG. 6: Results of numerical simulations of (1) with the exponential friction model and corresponding feedback gain $K = K_{\text{exp}}$. Dashed lines correspond to using the friction model (3)–(4). Solid lines correspond to replacing $\text{sgn}(\dot{x})$ with $\tanh(100\dot{x})$. Initial conditions used are as in (12) for various values θ_0 of the time delay, τ. The bottom graph shows a zoom in of the top graph.

Time Delay with the Dynamic Friction Model

The results for the dynamic friction model are similar to that for the exponential friction model. We briefly summarize them here. More detail can be found in [19]. Using linear stability analysis as above, we find that the critical time delay is $\tau_c \approx 0.1169$ seconds. Experimentally, we observed that the upright equilibrium point was asymptotically stable until $\tau = 0.009$. For $0.009 < \tau < 0.023$ the experimental system exhibited oscillations about the upright equilibrium point.For $\tau > 0.023$, the pendulum fell down.

The results of numerical simulations of the nonlinear model (1) with the delayed force (11) and the dynamic friction model (5)–(6) are summarized in top graph of Figure 7 with a zoom in shown in the bottom graph. These predictions are in reasonable agreement with the experimental observations. The simulations show that the effective critical delay increases as θ_0 decreases, limiting close to the theoretically predicted critical delay as θ_0 goes to zero. The simulations indicate that the discrepancy between the experimental observations and the theoretical prediction of the critical delay is because that the equilibrium point is only locally asymptotically stable.

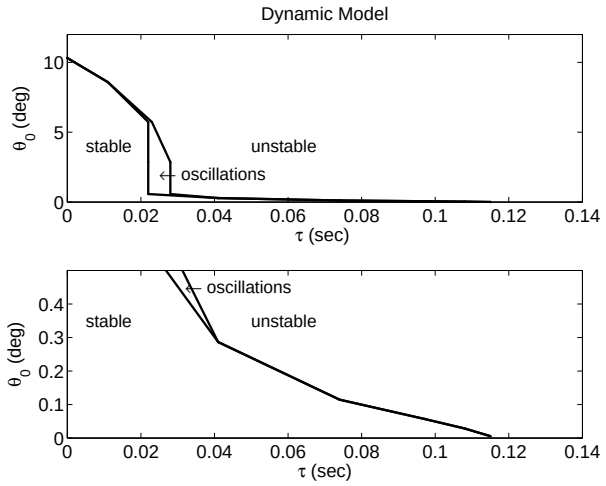

FIG. 7: Results of numerical simulations of the nonlinear system (1) with the dynamic friction model and corresponding feedback gain. Initial conditions used are as in (12) for various values θ_0 of the time delay, τ. The bottom graph shows a zoom in of the top graph.

DISCUSSION

We studied a model for an experimental pendulum system where feedback control is used to maintain the pendulum in the upright position. The main focus of our study was how the model for friction between the cart and the track affects the performance of the controller. Previous work used a simple viscous friction model to design the controller. This resulted in small amplitude oscillations when this controller was implemented in the experimental system. We gave a possible explanation of this behaviour by studying the situation when the controller designed using a simple viscous friction model is implemented in a model which incorporates stick slip friction. We considered two stick slip friction models: exponential and dynamic. We showed that the controller may fail (the equilibrium point is not linearly stable) or have bad performance (the equilibrium point is linearly stable, but has a small basin of attraction). The results depended on the model of stick slip friction used. With both stick slip friction models, numerical simulations revealed stable, small amplitude oscillations that are very similar to those observed in the experiment.

We then used each stick slip friction model to design a new controller for the system using the same LQR design as for the simple viscous friction model. Since the friction models contain nondifferentiable terms, this requires approximating these terms by smooth functions. This

idea has been applied before [20] to increase the efficiency of simulations of models with Coulomb friction, but we have not seen it applied to controller design. There is no theory to guarantee that a controller designed using such an approximation will stabilize the system. However, the controllers we designed based on approximations of either the exponential or dynamic friction model achieved stability of the system with only very low amplitude noise. We emphasize that we did no parameter tuning of the controller to achieve the excellent performance. Similar performance using friction compensation seems only to be achieved after careful parameter tuning [8].

Finally, we studied the effect of time delay in the feedback control. We found that a controller based on the dynamic friction model is slightly more robust to time delay (critical delay of 0.1169 seconds vs 0.1069 seconds). Both are more robust than a controller based on a simple viscous friction model (critical delay of 0.062 seconds [16]). Linear stability analysis of the model gave a poor prediction of the critical time delay observed in the experiment. A much better prediction was obtained from numerical simulations of the full nonlinear model. The reason for this is that the upright equilibrium point is locally stable and only initial conditions starting very close to the equilibrium point achieve stability. Since it is difficult to experimentally achieve initial conditions very close to the equilibrium point, the effective critical delay is smaller than that predicted by linear stability analysis.

The main conclusion of our work is that, when choosing a model to be used in designing a controller, it is critical not only to include friction but to include the correct type of friction model and to estimate the parameters as accurately as possible. For systems with stick slip friction, we found that both the exponential model [9] and the dynamic model of Canudas de Wit et al. [15] are adequate. Controllers based on either model stabilize the pendulum in the upright position. Both models have drawbacks. It is more difficult to calculate the controller for the model of [15] as it has an uncontrollable state. However, numerical simulations using the exponential model are difficult, due to the discontinuities in the model.

We leave to future work establishing whether/when a controller designed using a smooth approximation to a discontinuous nonlinearity stabilizes the discontinuous system. A promising tool for this is the stability theory for discontinuous systems established by Kuznetsov et al. [24]. Also of interest is the study of the bifurcation to periodic orbits which occurs when the feedback delay is sufficiently large. The periodic orbits are quite smooth, with few visible effects of the stick-slip friction, perhaps because the frequency is quite large. From

the numerical simulations, the bifurcation appears to be a subcritical Hopf. Proving this a nontrivial task, even for a system with smooth nonlinearities (e.g., [16]).

Acknowledgements

This research was supported by the Natural Sciences and Engineering Research Council (NSERC) of Canada, through the Discovery Grants and Undergraduate Summer Research Awards programs. The simulations were performed in the Matlab Simulink tool box using the solver `ode23tb`. We thank the reviewers their helpful comments and for pointing out several relevant references.

[1] Morris, K. A., and Juang, J. N., 1993. "Dissipative controller design for second-order dynamic systems". In Control of Flexible Structures, K. A. Morris, ed., AMS, pp. 71–90.

[2] Eltohamy, K. G., and Kuo, C. Y., Sep 1997. "Real time stabilisation of a triple link inverted pendulum using single control input". *Control Theory and Applications, IEE Proceedings -,* **144**(5), pp. 498–504.

[3] Olsson, H., and Åström, K. J., 2001. "Friction generated limit cycles". *IEEE Trans. Contr. Syst. Technol.,* **9**(4), pp. 629–636.

[4] Hirschorn, R. M., and Miller, G., 1999. "Control of nonlinear systems with friction". *IEEE Trans. Contr. Syst. Technol.,* **7**(5), pp. 588–595.

[5] Kollár, L. E., Stépán, G., and Hogan, S. J., 2000. "Sampling delay and backlash in balancing systems". *Periodica Polytechnica Ser. Mech. Eng.,* **44**(1), pp. 77–84.

[6] Bugeja, M., 2003. "Non-linear swing-up and stabilizing control of an inverted pendulum system". In Proceedings of the IEEE Region 8 EUROCON 2003: Computer as a Tool, B. Zajc and M. Tkalčič, eds., Vol. 2, IEEE, pp. 437–441.

[7] Medrano-Cerda, G. A., 1999. "Robust computer control of an inverted pendulum". *IEEE Cont. Sys. Mag.,* **19**(3), pp. 58–67.

[8] Fang, L., Chen, W. J., and Cheang, S. U., 2001. "Friction compensation for a double inverted pendulum". In Proceedings of the 2001 IEEE International Conference on Control Applications, pp. 908–913.

[9] Armstrong-Hélouvry, B., Dupont, P., and Canudas de Wit, C., 1994. "A survey of models, analysis tools and compensation methods for the control of machines with friction". *Automatica,* **30**(7), pp. 1083–1138.

[10] Chang, L.-H., and Lee, A.-C., July 2007. "Design of nonlinear controller for bi-axial inverted pendulum system". *Control Theory & Applications, IET,* **1**(4), pp. 979–986.

[11] van der Linden, G.-W., and Lambrechts, P. F., Aug 1993. "H_∞ control of an experimental inverted pendulum with dry friction". *IEEE Control Systems Magazine,* **13**(4), pp. 44–50.

[12] Neimann, H., and Poulsen, J. K., 2005. "Design and analysis of controllers for a double inverted pendulum". *ISA Transactions,* **44**, pp. 145–163.

[13] Yoshida, K., 1999. "Swing-up control of an inverted pendulum by energy-based methods". In Proceedings of the 1999 American Control Conference, Vol. 6, pp. 4045–4047.

[14] Jung, S., and Wen, J. T., 2004. "Nonlinear model predictive control for the swing-up of a rotary inverted pendulum". *J. Dyn. Sys. Meas. Control,* **126**(3), pp. 666–671.

[15] Canudas de Wit, C., Olsson, H., Åström, K. J., and Lischinsky, P., 1995. "A new model for control systems with friction". *IEEE Transactions on Automatic Control,* **40**(3).

[16] Landry, M., Campbell, S. A., Morris, K. A., and Aguilar, C., 2005. "Dynamics of an inverted pendulum with delayed feedback control". *SIAM J. Appl. Dyn. Sys.,* **4**(2), pp. 333–351.

[17] Stribeck, R., 1902. "Die wesentlichen eigenschaften der gleit- und rollenlage – the key qualities fo sliding and roller bearings". *Zeitschrift des Vereines Seutscher Ingenieure,* **46**, pp. 1342–1348,1432–1437.

[18] Armstrong-Hélouvry, B., 1991. *Control of Machines with Friction.* Kluwer, Boston.

[19] Campbell, S. A., Crawford, S., and Morris, K. A., 2007. "Time delay and feedback control of an inverted pendulum with stick slip friction". In Proceedings of the ASME 2007 International Design Engineering Technical Conferences (DECT2007).

[20] Haessig, D. A., and Friedland, B., 1991. "On the modeling and simulation of friction". *J. Dyn. Sys. Meas. Control,* **113**(3), pp. 354–362.

[21] Morris, K. A., 2001. *An Introduction to Feedback Controller Design.* Harcourt/Academic Press.

[22] Golubitsky, M., Stewart, I., and Schaeffer, D. G., 1988. *Singularities and Groups in Bifurcation Theory*, Vol. 2. Springer Verlag, New York.

[23] Kolmanovskii, V., and Nosov, V., 1986. *Stability of Functional Differential Equations*, Vol. 180

of *Mathematics in Science and Engineering*. Academic Press, London, England.

[24] Kuznetsov, Y. A., Rinaldi, S., and Gragnani, A., 2003. "One-parameter bifurcations in planar Filippov systems". *Int. J. Bifurc. Chaos,* **13**(8), pp. 2157–2188.